Journal Pre-proof

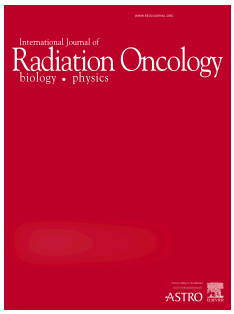

Quantitating Inter-fraction Target Dynamics during Concurrent Chemoradiation for Glioblastoma: A Prospective Serial Imaging Study

James Stewart, Ph.D, Arjun Sahgal, M.D, Young Lee, Ph.D., Hany Soliman, M.D., Chia-Lin Tseng, M.D., Jay Detsky, M.D. Ph.D., Zain Husain, M.D., Ling Ho, Sunit Das, M.D. Ph.D., Pejman Jabehdar Maralani, M.D., Nir Lipsman, M.D. Ph.D., Greg Stanisz, Ph.D., James Perry, M.D., Hanbo Chen, M.D., Eshetu G. Atenafu, M.Sc., Mikki Campbell, M.H.E. M.R.T(T)., Angus Z. Lau, Ph.D., Mark Ruschin, Ph.D., Sten Myrehaug, M.D.

PII: S0360-3016(20)34386-8

DOI: https://doi.org/10.1016/j.ijrobp.2020.10.002

Reference: ROB 26653

To appear in: *International Journal of Radiation Oncology • Biology • Physics*

Received Date: 11 August 2020

Revised Date: 18 September 2020

Accepted Date: 5 October 2020

Please cite this article as: Stewart J, Sahgal A, Lee Y, Soliman H, Tseng C-L, Detsky J, Husain Z, Ho L, Das S, Maralani PJ, Lipsman N, Stanisz G, Perry J, Chen H, Atenafu EG, Campbell M, Lau AZ, Ruschin M, Myrehaug S, Quantitating Inter-fraction Target Dynamics during Concurrent Chemoradiation for Glioblastoma: A Prospective Serial Imaging Study, *International Journal of Radiation Oncology • Biology • Physics* (2020), doi: https://doi.org/10.1016/j.ijrobp.2020.10.002.

Quantitating Inter-fraction Target Dynamics during Concurrent Chemoradiation for Glioblastoma: A Prospective Serial Imaging Study

James Stewart Ph.D[1]., Arjun Sahgal M.D[1,2]., Young Lee Ph.D. [2,3], Hany Soliman M.D. [1,2], Chia-Lin Tseng M.D. [1,2],Jay Detsky M.D. Ph.D. [1,2], Zain Husain M.D. [1,2], Ling Ho[1], Sunit Das M.D. Ph.D.[4,5,6], Pejman Jabehdar Maralani M.D.[7], Nir Lipsman M.D. Ph.D.[6,8,9], Greg Stanisz Ph.D.[8,10,11], James Perry M.D.[12], Hanbo Chen M.D. [1], Eshetu G Atenafu M.Sc.[13], Mikki Campbell M.H.E. M.R.T(T).[1], Angus Z Lau Ph.D.[8,10], Mark Ruschin Ph.D. [2,3], Sten Myrehaug M.D. [1,2]

[1]Department of Radiation Oncology, Sunnybrook Odette Cancer Centre, Toronto, Canada

[2]Department of Radiation Oncology, University of Toronto, Toronto, Canada

[3]Department of Medical Physics, Sunnybrook Odette Cancer Centre, Toronto, Canada

[4]Division of Neurosurgery and Centre for Ethics, St. Michael's Hospital, Toronto, Canada

[5]The Arthur and Sonia Labatt Brain Tumour Research Centre, SickKids Hospital, Toronto, Canada

[6]Division of Neurosurgery, University of Toronto, Toronto, Canada

[7]Department of Medical Imaging, University of Toronto, Sunnybrook Health Sciences Centre, Toronto, Canada.

[8]Physical Sciences, Sunnybrook Research Institute, Toronto, Ontario, Canada

[9]Harquail Centre for Neuromodulation, Sunnybrook Health Sciences Centre, Toronto, Ontario, Canada

[10]Department of Medical Biophysics, University of Toronto, Toronto, Ontario, Canada

[11]Department of Neurosurgery and Pediatric Neurosurgery, Medical University, Lublin, Poland

[12]Division of Neurology, Sunnybrook Health Sciences Centre, University of Toronto, Toronto, ON, Canada

[13]Department of Biostatistics, University Health Network, University of Toronto, Toronto, ON, Canada

Address for correspondence:
Sten Myrehaug, MD, FRCPC
Department of Radiation Oncology
Odette Cancer Centre, Sunnybrook Health Sciences Centre
2075 Bayview Avenue
Toronto, Ontario, CANADA
M4N 3M5
Phone: 1 416-480-4834
Fax: 1 416-480-6002
E-mail: sten.myrehaug@sunnybrook.ca

Statistical Analysis Author
Eshetu G Atenafu M.Sc.
Senior Biostatistician, University Health Network
610 University Avenue
Toronto, Ontario, CANADA
M5G 2C1
Phone: 1 416-946-2806
e.atenafu@utoronto.ca

Running title: Target dynamics during chemoradiation for glioblastoma

Conflict of Interest Statements:

Arjun Sahgal: Advisor/consultant: AbbVie, Merck, Roche, Varian, Elekta AB, BrainLAB, and VieCure; Board Member: International Stereotactic Radiosurgery Society (ISRS); Co-Chair: AO Spine Knowledge Forum Tumor; Past educational seminars: Elekta AB, Accuray Inc., Varian, BrainLAB, Medtronic Kyphon; Research grants: Elekta AB; Travel accommodations/expenses: Elekta AB, Varian, BrainLAB; Membership: Elekta MR Linac Research Consortium, Elekta Spine, Oligometastases and Linac Based SRS Consortia.

Hany Soliman: Travel accomodations/expenses: Elekta AB; Honoraria: Elekta AB. None related to this work.

Chia-Lin Tseng: Travel accommodations/expenses: Elekta AB; Honoraria: Elekta AB, and belongs to the Elekta MR-linac Research Consortium.

Sunit Das: Advisor/consultant: AbbVie, Xpan Medical, Synaptive; Board Member: Subcortical Surgery Group; Past educational seminars: AbbVie, Subcortical Surgery Group, Congress of Neurological Surgeons, American Association of Neurological Surgeons, Society for Neuro-Oncology; Research grants: Alkerme, Medicenna; Travel accommodations/expenses: Subcortical Surgery Group, Congress of Neurological Surgeons, American Association of Neurological Surgeons, Society for Neuro-Oncology, Integra. None related to this work.

Nir Lipsman: Grants from InSightec, personal fees and non-financial support from Focused Ultrasound Foundation, outside the submitted work.

Mikki Campbell: Honoraria: Elekta AB; research grants: Elekta AB; travel accommodations/expenses: Elekta AB. Mikki Campbell also belongs to the Elekta MR Linac Research Consortium.

Mark Ruschin: Co□inventor/owns associated intellectual property specific to the image□guidance system on the Gamma Knife Icon. None related to this work.

Sten Myrehaug: Research support: Novartis AG; Honoraria from Novartis AG and Ipsen and travel accomodations/expenses: Elekta. None related to this work.

James Stewart, Young Lee, Jay Detsky, Zain Husain, Ling Ho, Pejman Jabehdar Maralani, Greg Stanisz, James Perry, and Hanbo Chen, Eshetu Atenafu and Angus Lau report no conflict of interest.

Clinical Trial Information

Prospective Serial Imaging Study. Approved by Sunnybrook Health Sciences Research Ethics Board. Project Identification Number: 430-2015.

Funding Statement

This trial was funded by the Department of Radiation Oncology, Sunnybrook Odette Cancer Centre.

Data Sharing

All data specific to volume dynamic assessment as generated and analyzed during this study are included in the submitted article.

Abstract

Background: Magnetic Resonance Image-guided Radiotherapy (MRIgRT) has the potential to improve outcomes for glioblastoma (GBM) by adapting to tumor changes during RT. This study quantifies inter-fraction dynamics (tumor size, position, and geometry) based on sequential MRIs obtained during standard 6 week chemoradiation (CRT).

Methods: Sixty-one patients were prospectively imaged with gadolinium-enhanced T1 (T1c) and T2/FLAIR axial sequences at planning (Fx0), fraction 10 (Fx10), fraction 20 (Fx20), and one-month post CRT (P1M). Gross tumor volumes (GTV) and clinical target volumes (CTV) were contoured at all time points. Target dynamics were quantified by absolute volume (V), volume relative to Fx0 (V_{rel}), and the migration distance ($d_{migrate}$; the linear displacement of the GTV or CTV relative to Fx0). Temporal changes were assessed using a linear mixed effect model.

Results: Median V at Fx0, Fx10, Fx20, and at P1M for the GTV were 18.4 cm^3 (range: 1.1–110.5 cm^3), 14.7 cm^3 (range: 0.9-115.1 cm^3), 13.7 cm^3 (range: 0.6-174.2 cm^3) and 13.0 cm^3 (range: 0.9-76.3 cm^3), respectively, with corresponding median V_{rel} of 0.88, 0.77 and 0.71 at Fx10, Fx20 and P1M (relative to Fx0, $p < 0.001$ for all), respectively. The $GTVd_{migrate}$ and $CTVd_{migrate}$ at Fx10, Fx20 and P1M, were greater than 5 mm in 46%/54%, 50%/58%, and 52%/57% of patients, respectively. Dynamic tumour morphological changes were observed with 40% of patients exhibiting a decreased GTV volume ($V_{rel} \leq 1$) with a $d_{migrate} > 5$ mm during CRT.

Conclusions: Clinically meaningful tumor dynamics were observed during CRT for GBM, supporting evaluation of daily MRIgRT and treatment plan adaptation.

Keywords

Glioblastoma multiforme, tumor dynamics, magnetic resonance image-guided radiotherapy, intensity-modulated radiotherapy, adaptive replanning

Ethics Statement: This trial is approved by local institutional Research Ethics Board. Project Identification Number: xxx-xxxx

Introduction

Treatment for glioblastoma (GBM) remains challenging with 5-year overall survival (OS) rates remaining at ~5% despite aggressive therapy [1]. The standard of care for eligible patients following maximal surgical resection consists of 30 fractions of radiotherapy (RT) concurrent with temozolomide (TMZ), followed by maintenance monthly TMZ for 6 months [1]. While MRI is the gold standard for defining both target and organ-at-risk (OAR) structures at the time of RT planning [2, 3], the next clinical MRI is typically performed 4-6 weeks following RT completion. Image-based monitoring of a patient's tumor during RT is not a standard of care. Although there are limited studies evaluating inter-fraction MRI during a course of RT, they have typically been limited to a single imaging time point during the six weeks, and evaluated the predictive potential of functional imaging sequences without quantifying structural changes in tumor volumes [4-6].

Daily cone-beam CT (CBCT) linear accelerator image-guidance allows for bony anatomy matching to ensure precision of delivery, but does not permit soft tissue tumor visualization. With the advent of on-board MRI linear accelerators (MRL) [7, 8], the treatment paradigm is changing to daily tumor visualization. Our center has focused on developing a treatment protocol [9] for GBM with a 1.5T MRL (Elekta Unity, Elekta AB, Stockholm, Sweden). Our hypothesis was that significant inter-fraction changes in GBM tumor volume occur during a 6-week course of CRT, and that the assumption of modest geometric target changes may not hold true. The goal of this investigation was to quantify target volume changes during a 6-week standard fractionated RT course based upon a prospective sequential MRI research protocol. Such information is critical to inform techniques designed to improve the therapeutic ratio, such as smaller margins to account for uncertainty in delivery and the surrounding tissue at risk of microscopic disease extension [10-12], dose escalation [6, 13], and treatment adaptation to anatomical tumor volume changes [4, 14].

Methods and Materials

Patient characteristics and imaging

Sixty-one patients with GBM participated in this prospective research ethics board approved imaging trial. All patients had undergone maximal surgical resection or biopsy, and planned for a 6 week course of concurrent chemoradiation (CRT).

For clinical treatment, the gross tumor volume (GTV) was defined as the surgical resection cavity plus any residual enhancing tumor. The clinical target volume (CTV) was defined as a 1.5 cm isotropic expansion of the GTV respecting

anatomical barriers with the planning target volume (PTV) added as a 4 mm isotropic expansion to the CTV. All patients were treated with either 60 Gy (51/61) or 54 Gy (10/61) in 30 fractions delivered to the PTV. The imaging protocol included axial gadolinium enhanced T1-weighted (T1c) and T2/FLAIR volumetric MRIs at four time points: RT planning (Fx0), fractions 10 (Fx10) and 20 (Fx20) during CRT, and one-month post the last RT fraction (P1M). Patient characteristics are summarized in Table 1. The Fx0 MRI was acquired at a median of 19.5 days after surgery (range: 6-34 days); 52/61 (85%) patients had their Fx0 MRI between 10-20 days following surgery. The Fx10 MRI was acquired a median of 21 days after Fx0 (range: 15-29 days).

Thirteen of the 61 (21%) patients were imaged with a 3T Philips Achieva scanner (Philips Healthcare, Best, Netherlands) using post-Gadolinium T1-weighted (TR/TE = 9.5/2.3 ms; 0.49x0.49x1.50 mm voxels) and T2/FLAIR (TR/TE = 9000/125 ms; 0.43x0.43x5.00 mm voxels) sequences. The remaining 48 patients (79%) were imaged with a 1.5T Philips Ingenia system, again with a volumetric axial T1c (TR/TE = 6.2/4.7 ms; 0.50x0.50x1.00 mm voxels) and T2/FLAIR (TR/TE = 4800/291 ms; 0.56x0.56x2.00 mm voxels) sequences. The field strength of the second scanner (1.5T) matches that of the MRL currently treating patients at our institution [**Error! Reference source not found.**5]. All 61 patients completed the first three imaging sessions (Fx0, Fx10, and Fx20), and 54/61 (89%) went on to complete imaging at P1M. The P1M imaging time point does not explicitly capture inter-fraction target dynamics; it serves to put changes in context of a typical treatment response assessment scan.

Target definitions

At each time point, all target volumes were defined on T1c images using the Pinnacle treatment planning system (v. 9.8.0; Philips Medical Systems, Fitchburg, Wisconsin). In keeping with our institutional protocol and the recommendations of the MR-Linac International Consortium Research Group [16], the GTV was contoured as the surgical resection cavity plus any residual enhancing tumor. The CTV was defined as a 1.5 cm isotropic expansion of the GTV respecting anatomical barriers. All volumes were independently reviewed by a senior radiation oncologist (xx) to ensure consistency, and imported into the Monaco treatment planning system (Monaco Research v. 5.10; Elekta AB, Stockholm, Sweden) for analyses.

Tumor dynamics assessment

Target dynamics were quantified using the GTV and CTV contours from the Fx10, Fx20, and P1M image-datasets, all of which were rigidly co-registered to their respective Fx0 image. The following metrics were evaluated:

1) Absolute (V) and relative (V_{rel}) GTV and CTV: V_{rel} is defined as the absolute volume of the target at each time point relative to the respective Fx0 volume. V_{rel} decreases if V_{rel} is ≤ 1, and increases if V_{rel} is > 1.

2) Target migration distance ($d_{migrate}$): As outlined in Figure 1, $d_{migrate}$ is the maximum linear distance in any direction that the target departs from its respective Fx0 volume. The migration of the target volume was considered minor if $d_{migrate}$ was ≤ 5 mm and major if $d_{migrate}$ was > 5 mm. Eleven patients with presence of multifocal/multicentric disease foci at any timepoint were excluded from this calculation, leaving 50, 50, and 44 patients for analysis at Fx10, Fx20, and P1M, respectively. Combining the $d_{migrate}$ and V_{rel} yields four distinct combinations or morphologic changes that are illustrated in Figure 1(b).

The concept of $d_{migrate}$ was used to put into context morphological target changes relative to our margin concepts in RT. A 5 mm threshold was chosen to reflect internationally accepted planning target volume (PTV) expansions [17-18] to account for target motion and setup margin. In addition, a 5 mm $d_{migrate}$ for the GTV mirrors the intent to reduce margins within the academic community, as recently reported by a small margin phase 1/2 trial [12], and is intended to inform the design of our future protocol using the MRL.

Statistical Analysis

Linear mixed models were used to determine the relationship between target dynamics (GTV/CTV volumes and migration distances) and time, where time was considered as both a categorical and continuous variable. Time was also modelled as a fixed effect with random intercepts modelled for each patient to account for repeated measurements. Normality of the outcome measures were assessed using the Shapiro-Wilk test and, as a result of failing this test, V and $d_{migrate}$ for both the CTV and GTV were first log-transformed for stabilization. Linear mixed models were fit using the lme4 package (v1.1-21) and p-values were generated using the Satterthwaite method with the lmerTest package (v3.1-1) in the R statistical platform (v3.6.2). Logit-linked general linear mixed models were used to determine whether the proportion of patients with major $d_{migrate}$ (>5 mm) for each target changed over time as a categorical variable. Multinomial mixed logistic regression (Stata v15.1) was used to determine whether patients on average transitioned between the distinct morphologic categories (Figure 1(b)) over time. All linear mixed model parameter estimation was carried out with the maximal likelihood method. A p-value of 0.05 was used for statistical significance. No *a priori* sample number was calculated given this is an exploratory prospective study.

Results

Absolute and relative target volumes

As summarized in Figure 2(a), the median V for the GTV at Fx0 was 18.4 cm^3 (range: 1.1-110.5 cm^3, interquartile range (IQR): 27.6 cm^3) and decreased to 14.7 (range: 0.9-115.1 cm^3, IQR: 30.7 cm^3), 13.7 (range: 0.6-174.2 cm^3, IQR: 27.6

cm^3), and 13.0 (range: 0.9-76.3 cm^3, IQR: 24.5 cm^3) at Fx10, Fx20, and P1M, respectively. The median GTV V_{rel} were 0.88 (range: 0.34-1.40), 0.77 (range: 0.09-2.13) and 0.71 (range: 0.17-3.80) at Fx10, Fx20, and P1M, respectively. The GTV was observed to decrease for most patients at each time point as indicated in Figure 2(a): 44 (72%), 49 (80%), and 44 (81%) patients had a $V_{rel} \leq 1$ at Fx10, Fx20, and P1M, respectively. Relative to Fx0, this decrease was statistically significant at all three time points ($p<0.001$). Similarly, the decrease in V was statistically significant from Fx10 to both Fx20 and P1M ($p=0.013$ and $p=0.002$, respectively), but not from Fx20 to P1M ($p=0.46$).

The median V for the CTV also decreased over time. As detailed in Figure 2(b), the specific values were 114.6 cm^3 (range: 33.9-374.1 cm^3, IQR: 76.8 cm^3), 106.7 (range: 29.9-370.5 cm^3, IQR: 108.2 cm^3), 99.3 (range: 27.5-401.2 cm^3, IQR: 100.5 cm^3), and 101.7 (range: 30.3-376.0 cm^3, IQR: 87.3 cm^3) at Fx0, Fx10, Fx20, and P1M, respectively. The median CTV V_{rel} were 0.96 (range: 0.59-1.37), 0.88 (range: 0.41-1.63), and 0.86 (range: 0.39-2.38) at Fx10, Fx20, and P1M, respectively. Again, this decrease, relative to Fx0, was statistically significant at all time points ($p=0.027$, $p<0.0001$, and $p<0.0001$, respectively). The CTV volume decrease was also statistically significant from Fx10 to both Fx20 and P1M ($p=0.023$ and $p=0.008$, respectively), but not from Fx20 to P1M ($p=0.61$).

Target migration

The $d_{migrate}$ for the GTV and CTV are summarized for all patients in Figure 3. For the GTV, 23 (46%), 25 (50%), and 23 (52%) patients had a major $d_{migrate}$ (> 5 mm) at Fx10, Fx20, and P1M, respectively. The magnitude of the migration distance was particularly striking at the individual patient level; GTV $d_{migrate}$ was > 10 mm in 10 (20%), 8 (16%), and 8 (18%) and > 15 mm in 2 (4%), 3 (6%), and 4 (9%) patients at Fx10, Fx20, and P1M, respectively, and reached a maximum value of 17.3, 21.2, and 31.5 mm at the same time points, respectively. The $d_{migrate}$ for the CTV showed similar trends with 27 (54%), 29 (58%), and 25 (57%) patients having a $d_{migrate}$ > 5 mm at Fx10, Fx20, and P1M, respectively. The CTV $d_{migrate}$ was > 10 mm in 9 (18%), 6 (12%), and 8 (18%) and > 15 mm in 3 (6%), 1 (2%), and 4 (9%) of patients with maximum values of 16.2, 22.8, and 31.7 mm at Fx10, Fx20, and P1M, respectively. No statistically significant changes in the log-transformed $d_{migrate}$ with respect to time were observed for both the GTV and CTV ($p=0.32$ and $p=0.13$, respectively). Relative to Fx0, consequential inter-fraction migration distances are observed across the patient cohort. For example, as outlined in the right side plots of Figure 3, 58% and 66% of patients had a $d_{migrate}$ > 5 mm for the GTV and CTV, respectively, at either Fx10 or 20. Similarly, 26%/24% and 8%/8% of patients had a $d_{migrate}$ greater than 10 and 15 mm, respectively, for the GTV and CTV.

Correlation of target volumes and migration

The correlation between target volume changes and the migration distance for the GTV and CTV are summarized in Figure 4. The plots are segmented according to minor/major $d_{migrate}$ and increasing/decreasing V_{rel} as outlined in the schematic of Figure 1(b). A considerable number of patients had a major GTV migration ($d_{migrate}$ > 5 mm) even in the context of a decreasing GTV volume ($V_{rel} \leq 1$). Specifically, 10 (21%), 16 (33%), and 14 (34%) patients had both $V_{rel} \leq 1$ and $d_{migrate}$ > 5 mm at Fx10, Fx20, and P1M, respectively. Driven by these GTV dynamics, the CTV showed a similar trend: 16 (32%), 19 (38%), and 16 (36%) of patients had a major CTV $d_{migrate}$ with a decreasing CTV V_{rel} at Fx10, Fx20, and P1M, respectively. There were no statistically significant changes in the number of patients in, nor in crossover between, the four quadrants of Figure 4.

Illustrative representative relationships between the GTV V_{rel} and GTV $d_{migrate}$ for five individual patients are shown in Figure 5:

(a) The sole patient at any time point with an increasing GTV V_{rel} and minor $d_{migrate}$ (V_{rel} = 1.01 and $d_{migrate}$ = 4.5 mm at Fx10).

(b) The smallest V_{rel} for any patient at any time point as per a V_{rel} of 0.09 at Fx20. Though the non-Fx0 GTVs are entirely within the boundary of the Fx0 GTV on the depicted slice, the non-Fx0 GTV extends outside the Fx0 on other slices. As a result, $d_{migrate}$ was non-zero at each time point.

(c) A large GTV $d_{migrate}$ in the presence of a decreasing GTV volume (V_{rel} = 0.85 and $d_{migrate}$ = 17.2 mm at Fx20).

(d) The largest absolute and relative GTV volume observed in this patent cohort with a V/V_{rel} of 115.1 cm^3/1.40 and 174.2 cm^3/2.13 at Fx10 and Fx20, respectively. This GTV of this patient also had the largest Fx20 $d_{migrate}$ at 21.2 mm.

(e) The largest GTV migration distance observed at Fx10 with a $d_{migrate}$ of 17.3 mm.

Discussion

The concept of radiation target volumes for GBM continues to evolve with improved understanding of tumor biology and patterns of treatment failure, alongside advances in imaging modalities and radiation delivery systems. As a result, treatment volumes have shifted from whole brain radiotherapy, to partial brain radiotherapy, to IGRT-based conformal techniques or fractionated stereotactic radiotherapy. This shift is predicated on the re-evaluation of the CTV based upon treatment failure analysis [19-22], treatment related toxicity [23-25] and improved understanding of the peritumoral at risk volume [13, 26-29].

These insights motivate a re-evaluation of the PTV, the geometric construct which accounts for tumor motion/changes as well as margin for potential setup and image-verification error. Landmark studies evaluating radiation therapy outcomes from the European Organization for Research and Treatment of Cancer (EORTC) and the Radiation Therapy Oncology Group (RTOG) defined their treatment volume in a single or 2-phase fashion as GTV plus a 2-3 cm expansion to field edge [1, 30], while more contemporary treatment protocols typically define a PTV in terms of a CTV expanded by a 3-5 mm margin [17-18]. Recent consensus contouring recommendations from the MR-Linac International Consortium Research Group suggest a 1.5 cm expansion on GTV to define the CTV [16]. In addition to treatment of the peritumoral region at risk, these large volumetric expansions likely account for the majority of intra-fraction tumor dynamic changes. However, with the trend towards decreasing the CTV and PTV, there may be an unintended negative impact on target coverage based upon unrecognized tumor cavity dynamics in the absence of on-treatment MRI. As the PTV is a fixed planning objective, this study aimed to identify and quantify these cavity dynamic changes to better inform margin selection and design for adaptive RT strategies.

Individualized plan adaptation has the potential to improve outcomes. Such an approach has been limited by the need to image during RT with MRI which has not been practical to date. Dedicated MRIgRT systems have recently emerged into practice [7, 8, 31-33]; their application for brain tumors has been considered by our group as an area of development. Before clinical implementation, several predicate studies were designed to evaluate this technology [9, 34]. Whereas the predicate studies focused on technology evaluation, the present study was clinically focused, aimed at understanding the temporal tumor dynamics during CRT, which have not been well characterized in the literature. The present trial represents a comprehensive prospective series looking at sequential MRI at multiple timepoints during CRT with methods specifically designed to evaluate GBM target dynamics as the primary endpoint. Our results suggest that dynamic tumor changes are highly variable across a patient cohort, and substantial morphological changes occur even in the presence of target volume regression. Across the cohort, GTV and CTV migrations were greater than 5mm, 10mm, and 15mm in 58%, 24%, and 8% of patients, respectively at some point during CRT. Migration distances could not be robustly predicted by target volumes; approximately a third of patients at each time point had major GTV or CTV migration, even in the presence of a decreasing V_{rel}. These combined results imply that the implications for margin reduction are significant, and support inter-fraction MR imaging to ensure consistent target coverage.

Our results are consistent with the evidence to date evaluating tumor dynamics based upon a single mid-treatment MRI for patients receiving CRT for GBM. Compared with the pre-treatment MRI of 25 patients with newly diagnosed GBM,

Manon et al. observed that 80% of target volumes delineated on the mid-treatment scan would have had a geographic miss on the subsequent boost plan if it was assumed that the tumor volume does not change. Moreover, 27% were scored as a complete miss when defined as the portion of tumor beyond 2 cm of the initial GTV definition. Similarly, Tsien et al [6] performed an MRI at week 3 of CRT in 21 patients, with findings that support the observations of the current study that an overall decrease/stability in the GTV is seen during CRT. However, 25% of their cases showed an increase in the size of the GTV which dosimetrically would have led to a median under-dosing by the V95% by 10.8%. This group further evaluated functional diffusion maps and conventional radiologic response in a similar cohort, with MR imaging done at weeks 1 and 3 during treatment [35]. Kim and Lim [4] reported their dynamics study according to a CT at week 5 of CRT in 19 patients. Again, a trend towards a decrease in size of tumor volume was noted, with potential geographic miss of tumor in 26.3% of cases. Furthermore, these results are broadly in agreement with Mehta et al who in a preliminary cohort of 4 patients treated on the Viewray system (Oakwood Village, OH, USA), reported a general trend of cavity volume reductions during radiotherapy with an increase in edema observed in one of the four patients [36]. Collectively, the data suggest the potential for individualized tumor monitoring and treatment plan adaptation as an area to pursue. Our study substantially contributes to the existing body of literature by including analyses of a comprehensive cohort of patients, with a finer sampling of MR imaging time points to deepen our understanding of tumor dynamics. We note that the underlying mechanism causing changes in $d_{migrate}$ is multivariable; resolution of the surgical cavity, tumor progression (whether true or pseudo-progression), and normal central nervous system motion all potentially play a role. Future work as outcome data matures will evaluate these factors.

The clinical implications of these imaging findings are compelling. First, our observation that 58% and 68% of patients had a $d_{migrate}$ > 5mm for the GTV and CTV (Figure 3) suggests that with a trend towards a decrease in GTV/CTV volume, an isotropic volumetric margin of 3 to 5 mm for PTV is insufficient if to accommodate inter-fraction tumor dynamics. A significant proportion of patients would be potentially under-covered by the therapeutic RT dose, supporting the importance of inter-fraction plan adaptation to improve the accuracy of radiation delivery. Our data confirm that if we are to reduce the CTV, then it is critical to monitor these patients with MRIgRT during the 6 weeks of CRT to ensure target volume coverage. Recently, a 5 mm CTV with no PTV was applied to GBM patients in a Phase1/2 study for patients receiving a 5 fraction treatment course [12], with results indicating promise both in clinical outcome and patient convenience. However, the short course of the investigated RT regimen, and noted volume changes seen between radiation planning and fraction 10 in our study (relative to planning, GTV volume change of 59% - 137%), highlight the importance of soft tissue targeting

verification early in the fractionation schedule, when small treatment margins are utilized. Our planned clinical protocol is to apply a 5 mm CTV; however, in context of a 6 week course of CRT, with daily MRIgRT to an appropriate PTV with plan adaptation as changes in volume and migration distances are observed.

Second, as GTV and CTV dynamics are co-related, strategies to adapt to changes in GTV morphology during RT will translate to improved coverage of the CTV. Given that the predominant pattern of volume change was a reduction in the GTV and CTV volumes (Figure 2) and the majority experience a decreasing Vrel with a minor $d_{migrate}$ (Figure 4), the therapeutic impact of adaptive radiotherapy as the GTV shrinks will translate to a reduction in the volume of brain irradiated. As recently evaluated in a randomized trial [21], irrespective of the definition of CTV, the majority of clinical failures are seen within the 95% treatment isodose volume. Although analysis was limited by the absence of reported molecular features, using a smaller treatment volume approach resulted in significant improvements in PFS and OS and statistically superior quality of life outcomes. This study raises a serious question as to the deleterious effect of radiation in large volume therapy. Therefore, we surmise the potential to improve GBM patient outcomes by incorporating MRIgRT and adaptive RT to allow for safe reduction in treatment volumes. It is important to be mindful that a common pattern of volume and migration change was an increase in V_{rel} with a major $d_{migrate}$ (Figure 4); in this worst-case clinical scenario there is potential to improve outcomes in these patients with MRIgRT adaptive RT as the dosimetric implications of small margin non-adaptive RT would likely be significant.

Third, from Figure 2, the volume regression data quantified in this study suggests that the majority of target changes occur between Fx0 and Fx10, with no statistically significant change between Fx20 and P1M. Between the Fx0 and Fx10, absolute T1c GTV changed by a range of -33.2 to +33.2 cm^3. Similarly, the GTV and CTV migration distance reached as high as 17.3 and 16.2 mm, respectively. These observations may be related to evolving post-operative and RT related changes dominant earlier in the course, as opposed to tumor related cellular changes likely more reflective of the later dynamics observed between Fx10 to Fx20. An initially identified driver of inter-fraction changes is the extent of surgical resection. A preliminary analysis of surgical extent with respect to target dynamics suggests that patients who underwent subtotal resection or biopsy had larger GTV volumes at planning, and higher V_{rel} and $d_{migrate}$ during CRT (data not shown). This relationship, and other clinical and biologic factors which may influence cavity dynamics will be subject to further evaluation. In addition, the prognostic implications of the observed tumor dynamics at each time point will be reported as the outcome data mature to better inform these hypotheses. We chose to image at Fx20 as our second time point to allow sufficient time for potential observed volume changes to manifest, but also to provide significant time to allow for

meaningful plan adaptation. Ultimately, the ideal time points for imaging will be better clarified as we analyze our daily MRIgRT with the MRL.

The central limitation of this study is the number of imaging time points; our observations will be validated and refined with daily images acquired on the MRL. Further limitations include the lack of dosimetric evaluation associated with these observed changes in context with known prognostic molecular features and treatment failure analysis, which is a specific future study direction of this patient cohort. While this study focused on T1c MRI to inform PTV margins, future direction with this patient cohort involve the utilization of multiparametric sequences, including chemical exchange saturation transfer (CEST) [37], magnetization transfer (MT) [38] and apparent diffusion coefficient (ADC) [27, 28], to inform the peritumoral CTV as opposed to a standard volumetric expansion. Online MR guided radiotherapy also enables the possibility of rapidly responding to high-risk tumor volumes identified by on-treatment functional imaging.

Conclusion

Clinically meaningful tumor dynamics were observed during chemoradiation for glioblastoma, which may have significant implications on appropriate treatment volume margins, and support the adoption of MR-guided radiotherapy. Ultimately, by incorporating and adapting to functional information and inter-fraction structural changes, patient-specific target definition and accuracy can be increased. The fundamental challenge is how to utilize these imaging and adaptation processes to improve the therapeutic ratio by developing techniques based on margin reduction or hypofractionation.

References

[1] Stupp R, Mason W, van den Bent MJ, et al. Radiotherapy plus concomitant and adjuvant temozolomide for glioblastoma. New England Journal of Medicine, 2005; 352(10)987-996.

[2] Dhermain FG, Hau P, Lanfermann H, Jacobs AH, and van den Bent MJ. Advanced MRI and PET imaging for assessment of treatment response in patients with gliomas. The Lancet Neurology, 2010;9(9):906–920.

[3] Fiorentino A, Caivano R, Pedicini P, and Fusco V. Clinical target volume definition for glioblastoma radiotherapy planning: magnetic resonance imaging and computed tomography. Clinical and Translational Oncology, 2013;15(9):754–758.

[4] Kim TG and Lim DH. Interfractional variation of radiation target and adaptive radiotherapy for totally resected glioblastoma. Journal of Korean Medical Science. 2013;28(8):1233–1237.

[5] Manon R, Hui S, Chinnaiyan P, et al. The impact of mid-treatment MRI on defining boost volumes in the radiation treatment of glioblastoma multiforme. Technology in Cancer Research & Treatment. 2004;3(3):303-307

[6] Tsien C, Gomez-Hassan D, Ten Haken RK, et al. Evaluating changes in tumor volume using magnetic resonance imaging during the course of radiotherapy treatment of high-grade gliomas: Implications for conformal dose-escalation studies. International Journal of Radiation Oncology Biology Physics, 2005;62(2):328–332.

[7] Hall WA, Paulson ES, van der Heide UA, et al. The transformation of radiation oncology using real-time magnetic resonance guidance: A review. European Journal of Cancer, 2019;122:42-52.

[8] Cao Y, Tseng CL, Balter JM, Teng F, Parmar HA, and Sahgal A. MR-guided radiation therapy: transformative technology and its role in the central nervous system. Neuro-oncology, 19(Suppl. 2):ii16–ii29, 2017.

[9] xxxxxx

[10] Gebhardt BJ, Dobelbower MC, Ennis WH, Bag AK, Markert JM, and Fiveash JB. Patterns of failure for glioblastoma multiforme following limited-margin radiation and concurrent temozolomide. Radiation Oncology. 2014;9(1):130.

[11] Tsien C, Moughan J, Michalski JM, et al. Phase I three-dimensional conformal radiation dose escalation study in newly diagnosed glioblastoma: Radiation Therapy Oncology Group Trial 98-03. International Journal of Radiation Oncology Biology Physics. 2009;73(3):699–708.

[12] Azoulay M, Chang SD, Gibbs IC, et al. A phase 1/2 trial of 5-fraction stereotactic radiosurgery with 5 mm margins with concurrent and adjuvant temozolomide in newly diagnosed glioblastoma: primary outcomes. Neuro-Oncology (in press), 2020.

[13] Tsien CI, Brown D, Normolle D, et al. Concurrent temozolomide and dose-escalated intensity-modulated radiation therapy in newly diagnosed glioblastoma. Clinical Cancer Research, 2012;18(1):273–279.

[14] Pirzkall A, McGue C, Saraswathy S, et al. Tumor regrowth between surgery and initiation of adjuvant therapy in patients with newly diagnosed glioblastoma. Neuro-oncology. 2009;11(6):842–852.

[15] Lagendijk JJW, Van Vulpen M, and Raaymakers BW. The development of the MRI linac system for online MRI-guided radiotherapy: a clinical update. Journal of Internal Medicine. 2016;280(2):203–208.

[16] Tseng CL, Stewart J, Whitfield G, et al. Glioma consensus contouring recommendations from a MR‐Linac International Consortium Research Group and evaluation of a CT-MRI and MRI−only workflow. Journal of Neuro-Oncology. 2020.

[17] Niyazi M, Brada M, Chalmers AJ, et al. ESTRO-ACROP guideline “target delineation of glioblastomas”. Radiotherapy and oncology, 2016;118(1):35-42.

[18] Cabrera AR, Kirkpatrick JP, Fiveash JB, et al. Radiation therapy for glioblastoma: executive summary of an American Society for Radiation Oncology evidence-based clinical practice guideline. Practical Radiation Oncology. 2016;6(4):217-225.

[19] Minniti G, Amelio D, Amichetti M, et al. Patterns of failure and comparison of different target volume delineations in patients with glioblastoma treated with conformal radiotherapy plus concomitant and adjuvant temozolomide. Radiotherapy & Oncology. 2010;97(3):377-381.

[20] Chang EL, Akyurek S, Avalos T, et al. Evaluation of peritumoral edema in the delineation of radiotherapy clinical target volumes for glioblastoma. International Journal of Radiation Oncology Biology Physics. 2007;68(1):144-150.

[21] McDonald MW, Shu HK, Curran WJ Jr, Crocker IR. Pattern of failure after limited margin radiotherapy and temozolomide for glioblastoma. International Journal of Radiation Oncology Biology Physics. 2011;79(1):130-136.

[22] Kumar N, Kumar R, Sharma SC, et al. Impact of volume of irradiation on survival and quality of life in glioblastoma: a prospective, phase 2, randomized comparison of RTOG and MDACC protocols. Neuro-Oncology Practice. 2020;7(1):86-93.

[23] Lawrence YR, Wang M, Dicker AP, et al. Early toxicity predicts long-term survival in high-grade glioma. British Journal of Cancer. 2011;104(9):1365-1371.

[24] Prust MJ, Jafari-Khouzani K, Kalpathy-Cramer J, et al. Standard chemoradiation for glioblastoma results in progressive brain volume loss. Neurology, 2015;85(8), 683-691.

[25] Bergo E, Lombardi G, Guglieri I, Capovilla E, Pambuku A, and Zagone V. Neurocognitive functions and health-related quality of life in glioblastoma patients: a concise review of the literature. European journal of cancer care. 2019;28(1), e12410.

[26] Wahl DR, Kim MM, Aryal MP, et al. Combining perfusion and high B-value diffusion MRI to inform prognosis and predict failure patterns in glioblastoma. International Journal of Radiation Oncology Biology Physics. 2018;102(4):757-764.

[27] Jena R, Price SJ, Baker C, et al. Diffusion tensor imaging: possible implications for radiotherapy treatment planning of patients with high-grade glioma. Clinical Oncology. 2005;17(8):581-590.

[28] Jeong D, Malalis C, Arrington JA, Field AS, Choi JW, Kocak M. Mean apparent diffusion coefficient values in defining radiotherapy planning target volumes in glioblastoma. Quantitative Imaging in Medicine and Surgery. 2015;5(6):835-845.

[29] Harat M, Małkowski B, Makarewicz R. Pre-irradiation tumour volumes defined by MRI and dual time-point FET-PET for the prediction of glioblastoma multiforme recurrence: A prospective study. Radiotherapy and Oncology. 2016;120(2):241-247.

[30] Gilbert MR, Dignam JJ, Armstrong TS, et al. A randomized trial of bevacizumab for newly diagnosed glioblastoma. New England Journal of Medicine. 2014;370(8):699-708.

[31] Mutic S and Dempsey JF. The ViewRay system: Magnetic resonance–guided and controlled radiotherapy. Seminars in Radiation Oncology. 2014;24(3):196–199.

[32] Fallone BG. The rotating biplanar linac–magnetic resonance imaging system. Seminars in Radiation Oncology. 2014;24(3):200–202.

[33] Jaffray DA, Carlone MC, Milosevic MF, et al. A facility for magnetic resonance–guided radiation therapy. Seminars in Radiation Oncology, 2014;24(3):193–195.

[34] Tseng CL, Eppinga W, Seravalli E, et al. Dosimetric feasibility of the hybrid Magnetic Resonance Imaging (MRI)-linac System (MRL) for brain metastases: The impact of the magnetic field. Radiotherapy and Oncology, 2017;125:273-279.

[35] Hamstra DA., Galbán, CJ, Meyer CR, et al. Functional diffusion map as an early imaging biomarker for high-grade glioma: correlation with conventional radiologic response and overall survival. Journal of clinical oncology.2008;26(20), 3387.

[36] Mehta S, Gajjar SR, Padgett KR, et al. Daily tracking of glioblastoma resection cavity, cerebral edema, and tumor volume with MRI-guided radiation therapy. Cureus. 2018;10(3):e2346.

[37] Mehrabian H, Desmond KL, Soliman H, Sahgal A, and Stanisz GJ. Differentiation between radiation necrosis and tumor progression using chemical exchange saturation transfer. Clinical Cancer Research. 2017;23(14):3667-3675.

[38] Mehrabian H, Myrehaug S, Soliman H, Sahgal A, and Stanisz GJ. Quantitative magnetization transfer in monitoring glioblastoma (gbm) response to therapy. Scientific Reports. 2018;8(1):2475.

Figure Captions

Fig 1: (a) Schematic illustration of the migration distance ($d_{migrate}$). The migration distance is the maximum linear distance (in three-dimensions) the target – either the GTV or CTV - deviates from its original Fx0 volume. In the illustration, the GTV at planning (Fx0; unfilled circle) and the GTV at a later timepoint (FxX; shaded ellipse) are depicted. (b) Combining minor ($d_{migrate} \leq 5$ mm) and major ($d_{migrate} > 5$ mm) migration distances with decreasing ($V_{rel} \leq 1$) and increasing ($V_{rel} > 1$) relative target volumes yields four distinct combinations as illustrated.

Fig 2: Summary of GTV (a) and CTV (b) absolute (V) and relative (V_{rel}) changes. The violin plot at each time point in each subfigure delineates individual patient volumes (scatter points), probability density estimate (shaded region), mean (white line), and median (black line). The labelled outlier is depicted in detail in Figure 5(d).

Fig 3: GTV (a) and CTV (b) migration distance ($d_{migrate}$) analysis. Eleven patients with 2 or more disease foci at any time point were excluded, leaving n = 50, 50, and 44 at Fx10, Fx20, and P1M. Left column: The violin plot at each time point delineates $d_{migrate}$ for each patient (scatter points), symmetrical probability density estimate (shaded region), mean (white line), and median (black line). The outlier patients of the labelled scatter points are depicted in detail in Figure 5. Right column: Cumulative proportion of patients with the given $d_{migrate}$ during radiotherapy; only Fx10 and Fx20 are included to

emphasize inter-fraction effects. For example, 58% and 66% of patients in this study had a $d_{migrate}$ > 5 mm for the GTV and CTV, respectively, at Fx10 and/or Fx20.

Fig 4: Relationship between the GTV (a) and CTV (b) migration distance ($d_{migrate}$) and respective relative volume (V_{rel}) at Fx10 (left column), Fx20 (middle column), and P1M (right column). Individual points delineate the migration distance and relative volume of a single patient. Eleven patients with 2 or more disease foci at any time point were excluded, leaving a total of n = 50, 50, and 44 at Fx10, Fx20, and P1M, respectively. The labelled outliers are illustrated in further detail in the respective subfigure of Figure 5.

Fig 5: Axial slices of five patients at Fx0, Fx10, Fx20 and P1M illustrating patient-specific serial GTV changes. The Fx0 GTV is denoted in white; this contour is also interpolated post-registration to non-planning (Fx10, Fx20, and P1M) images for comparison purposes (due to this interpolation, this contour may appear slightly different on the non-planning images). The GTV at Fx10, Fx20, and P1M is shown in red.

Table 1: Patient Characteristics

Variable	**N=61**
Median Age in Years (Range)	56 (19-69)
Sex	
Male	38 (62%)
Female	23 (38%)
Resection Type	
Gross Total	18 (30%)
Subtotal	35 (57%)
Biopsy	8 (13%)
Tumor Location	
Frontal	17 (28%)
Parietal	11 (18%)
Temporal	24 (39%)
Occipital	3 (5%)
Thalamus	5 (8%)
Cerebellum	1 (2%)
MGMT (O6-methylguanine-DNA methyl-transferase) status	
Methylated	24 (39%)
Unmethylated	27 (44%)
Unknown	10 (16%)
IDH-1 (Isocitrate dehydrogenase 1) Status	
Mutant	3 (5%)
Wild-Type	57 (93%)
Unknown	1 (2%)
Median Days from Surgery to Pre-Treatment (Fx0) MRI (Range)	19.5 (6-34)

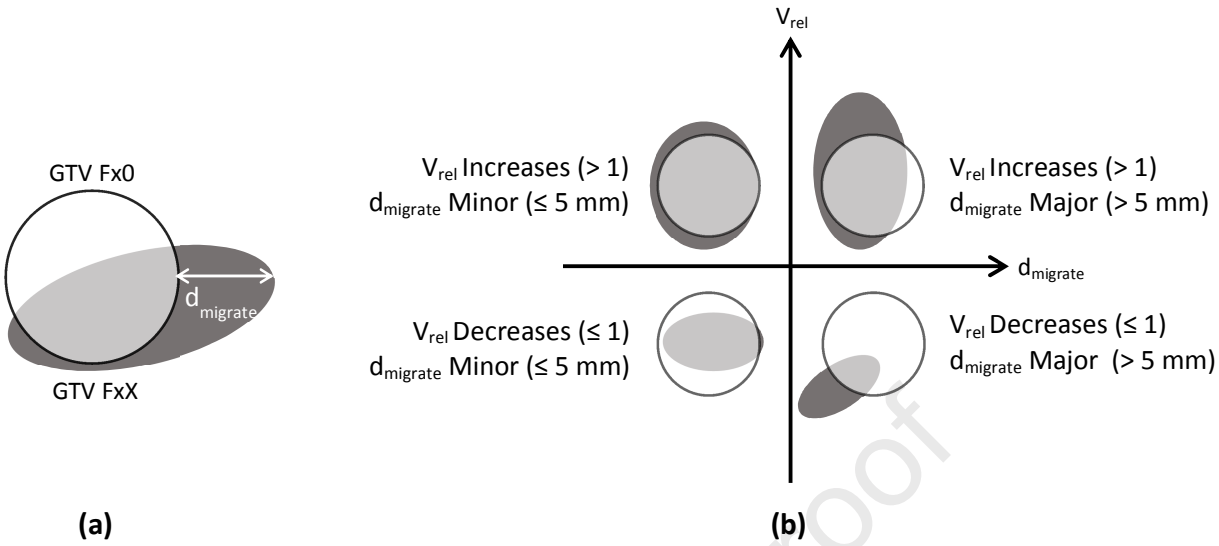

Figure 1: Schematic illustration of the migration distance ($d_{migrate}$).

Figure 2: GTV and CTV Absolute and Relative Volume Changes

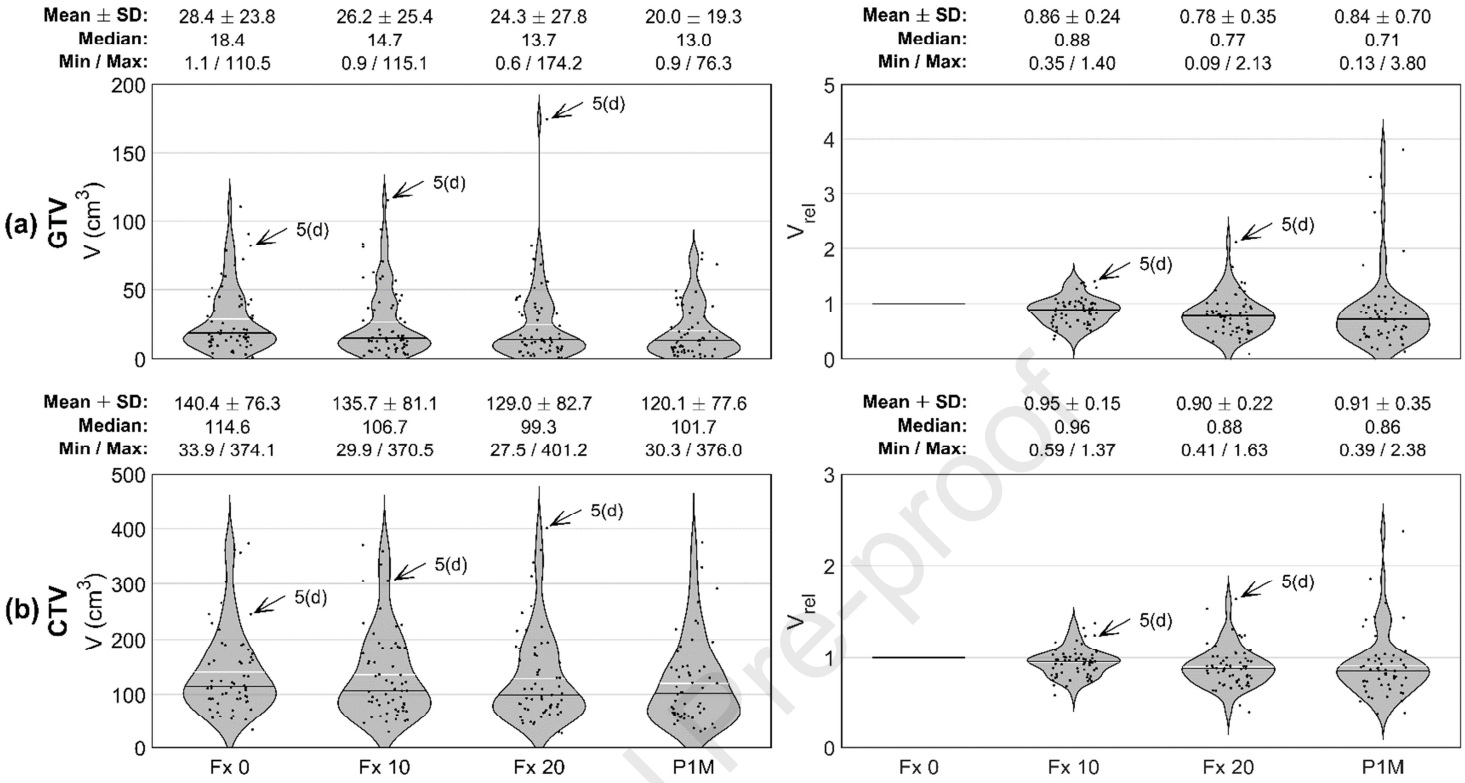

Figure 3: GTV and CTV Migration Distance ($d_{migrate}$) Analysis

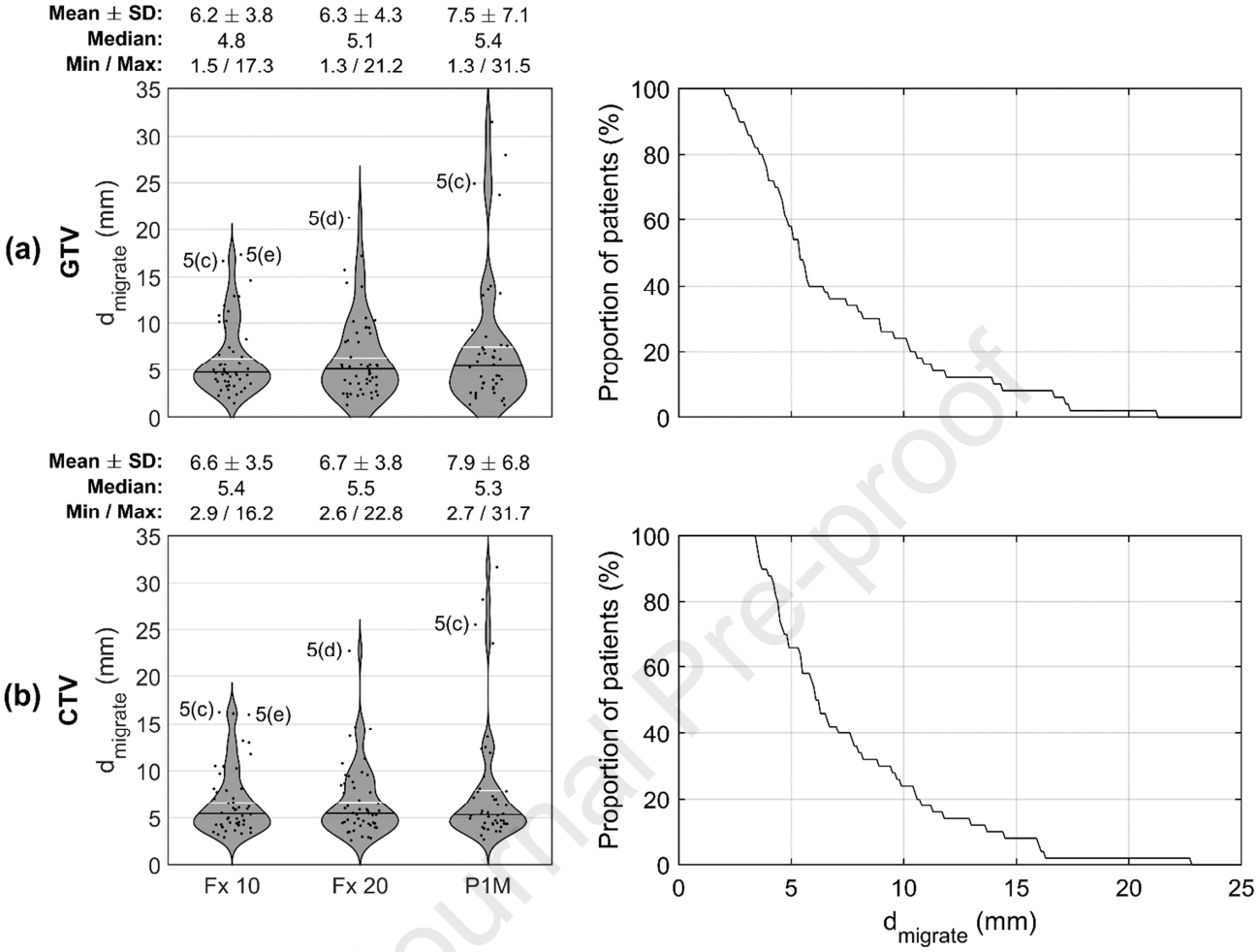

Figure 4: Relationship Between the GTV and CTV Migration Distance Relative Volume at Each Timepoint.

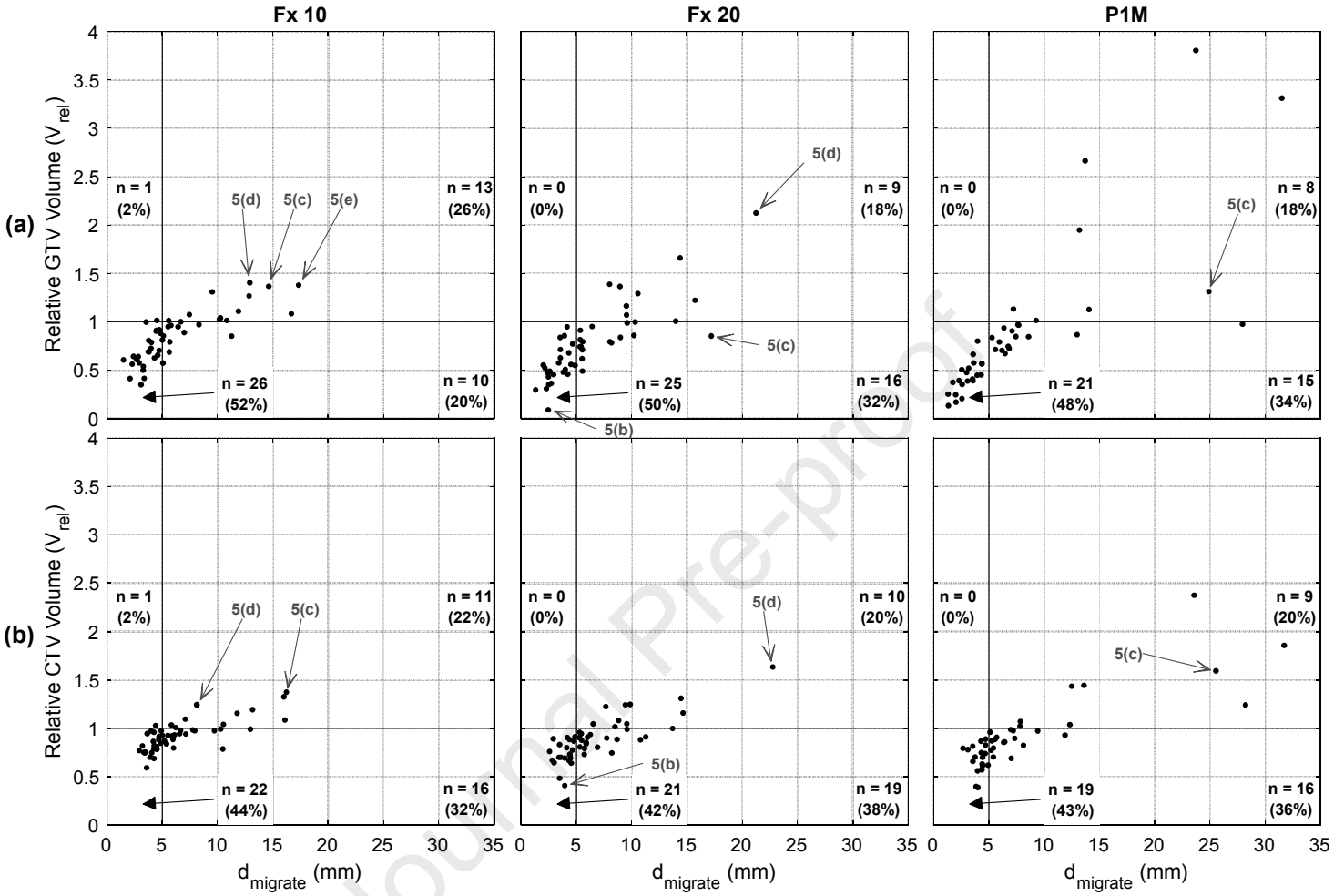

Figure 5: Illustrative Patient-Specific Serial GTV Changes